Dynamics of vortex–antivortex pair in a superconducting thin strip with narrow slits*

An He(何安)[1,†], Cun Xue(薛存)[2], and You-He Zhou(周又和)[3,4]

[1] College of Science, Chang'an University, Xi'an 710064, China
[2] School of Mechanics, Civil Engineering and Architecture, Northwestern Polytechnical University, Xi'an 710072, China
[3] School of Aeronautics, Northwestern Polytechnical University, Xi'an 710072, China
[4] Key Laboratory of Mechanics on Disaster and Environment in Western China attached to the Ministry of Education of China, and Department of Mechanics and Engineering Sciences, Lanzhou University, Lanzhou 730000, China

(Received 4 November 2016; revised manuscript received 23 January 2017; published online 10 March 2017)

In the framework of phenomenological time-dependent Ginzburg–Landau (TDGL) formalism, the dynamical properties of vortex–antivortex (V-Av) pair in a superconductor film with a narrow slit was studied. The slit position and length can have a great impact not only on the vortex dynamical behavior but also the current–voltage (I–V) characteristics of the sample. Kinematic vortex lines can be predominated by the location of the slit. In the range of relatively low applied currents for a constant weak magnetic field, kinematic vortex line appears at right or left side of the slit by turns periodically. We found such single-side kinematic vortex line cannot lead to a jump in the I–V curve. At higher applied currents the phase-slip lines can be observed at left and right sides of the slit simultaneously. The competition between the vortex created at the lateral edge of the sample and the V-Av pair in the slit will result in three distinctly different scenarios of vortex dynamics depending on slit length: the lateral vortex penetrates the sample to annihilate the antivortex in the slit; the V-Av pair in the slit are driven off and expelled laterally; both the lateral vortex and the slit antivortex are depinned and driven together to annihilation in the halfway.

Keywords: vortex–antivortex pair, phase-slip line, current–voltage characteristic, narrow slit

PACS: 74.78.Na, 73.23.–b, 74.40.–n, 85.25.–j **DOI:** 10.1088/1674-1056/26/4/047403

1. Introduction

With the progress of modern microfabrication techniques, the electronic properties of mesoscopic superconducting samples has attracted much attention.[1] The vortex matter of such structures in an external field is strongly influenced by the geometry and size of the sample.[2–4] Over the past decades, electric-field-induced flux flow instabilities have been intensively considered both in low-temperature and high-temperature superconductors.[5–9] Since the discovery of the steplike features in the current–voltage characteristics of superconductor, phase-slip phenomenon has well explained such an effect.[10] In two-dimensional (2D) superconductors the variations of the order parameter may not necessarily uniform along the phase-slip line (PSL) perpendicular to the applied current.[11] Numerical simulations have first observed the oscillations of the order parameter along the PSL using the 2D time-dependent Ginzburg–Landau (TDGL) equations,[12] and the existence of kinematic vortices was reported by the experimental evidence.[13] The very high velocity of kinematic vortices[13] compared to the maximal speed of Abrikosov vortices[14] leads to a rearrangement of the vortex lattice and a transition from slow to fast vortex motion (PSL) for an infinitely long superconducting slab placed in a parallel magnetic field.[15]

Vortex–antivortex (V-Av) state was first predicted to exist in mesoscopic superconducting squares and triangles as a consequence of the symmetry of the sample.[16,17] Geurts *et al.* reported the possibility to enhance the V-Av pair by placing strategically artificial pinning.[18–20] Moreover, the mechanism of nucleation of V-Av pairs generated by inhomogeneous field were presented.[21] The enhancement of superconductivity was achieved by constructing the hybrid superconductor-ferromagnetic structures.[22] Milošević *et al.*[23–26] systematically investigated the nucleation of V-Av pair by an array of magnetic dipoles.

Within the framework of time-dependent Ginzburg–Landau formalism, Berdiyorov *et al.*[27] proposed the tunable kinematics of PSLs in a superconducting stripe with magnetic dots. The guidance of kinematic V-Av pairs in a SC film by a magnetic bar and pattern formation of moving vortices were reported.[28,29] The superconducting critical parameters can be enhanced and modulated by arrays of magnetic dots,[30,31] and the influence of magnet size and magnetization on the magnetically engineered field-induced superconductivity was experimentally presented.[32,33] Silhanek *et al.*[34,35] experimentally

*Project supported by the Fundamental Research Funds for the Central Universities, China (Grant Nos. 310812171011 and G2016KY0305), the National Natural Science Foundation of China (Grant No. 11421062), and the National Key Project of Magneto-Constrained Fusion Energy Development Program, China (Grant No. 2013GB110002).

†Corresponding author. E-mail: hean@chd.edu.cn

© 2017 Chinese Physical Society and IOP Publishing Ltd

probed the V-Av dynamics and field-polarity-dependent flux creep in superconductor/ferromagnet hybrid structures. The stray field of applied current can generate V-Av pairs and move under the action of Lorentz force. Many studies have focused on the dynamics of V-Av pairs in a SC loop.[36–38]

Furthermore, Berdiyorov *et al.*[39] proposed a system of rectification in a broad and tunable frequency range by pining an Abrikosov vortex nearby the Josephson junction. Jelić *et al.*[40] reported the dynamical pinning induced by optical excitations can influence the vortex dynamics by tuning the amplitude and frequency in the real tunable system. Very recently, they[41] reported the velocimetry of superconducting vortices applying stroboscopic resonances. Besides, Carapella *et al.*[42,43] studied the current driven transition from Abrikosov-Josephson to Josephson-like vortex in mesoscopic lateral S/S'/S superconducting weak links.

Recently, we reported the guidance of kinematic vortices in the SC strip with artificial defects.[44] The effect of titled angle of slit on the vortex dynamics and *I*–*V* characteristics were studied. The dissipative states of superconducting samples with a periodic array of holes were experimentally measured.[45,46] It is also of great importance to investigate the influence of slit position and length on the kinematics of phase-slip lines in the sample with artificial defects. Therefore, in the present paper we studied the position-dependent resistive properties of the sample with one narrow slit. The paper is organized as follows. In Section 2, our model system and theoretical approach is presented. In Subsection 3.1, we show the repercussions of the slit position on the resistive state of the sample in the absence of magnetic field. In Subsection 3.2, we show the effect of slit length on the current-voltage characteristics under a weak magnetic field. Moreover, we can observe three distinct scenarios of dynamical behaviors of V-Av pairs by tuning slit length. Our main conclusions are given in Section 4.

2. Model system and theoretical approach

We consider a thin (thickness $d \ll \xi, \lambda$) superconducting strip (length L, width W see Fig. 1(a)) in the presence of transport current I through normal-metal contact of size a and magnetic field along the z axis perpendicular to the strip. A centered slit (length S_a and width S_b) is situated in the strip, and in another case d_s denotes the distance is shifted from the center. The vector plot in Fig. 1(b) shows the distribution of the superconducting current, in which larger arrows or smaller arrows regions correspond to high or low currents. The corresponding magnetic-field profile is superimposed and a pair of positive and negative flux is observed in the slit (white dashed line).

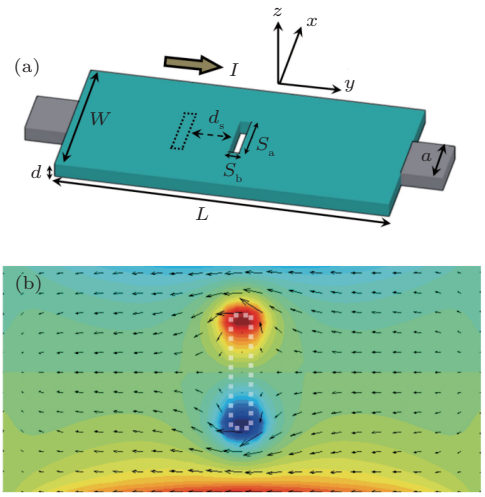


Fig. 1. (color online) (a) Schematic view of the superconducting sample (size $W \times L \times d$) contained a narrow slit (size $S_a \times S_b$) with attached normal leads (size a) in the presence of a dc current I along y axis. d_s denotes the shift distance of the slit from the center in another case. (b) Vector plot of the superconducting current in case of $H = 0$ and nonzero applied current. Larger (smaller) arrows regions corresponds to high (low) currents. The magnetic-field profile is superimposed and a pair of positive and negative flux is observed around the two tips of the slit (white dashed line).

To explore the dynamic properties of the deformed superconducting condensate, the generalized TDGL equation can be written in the following form[47,48]

$$\frac{u}{\sqrt{1+\gamma^2|\psi|^2}}\left(\frac{\partial}{\partial t}+\mathrm{i}\varphi+\frac{\gamma^2}{2}\frac{\partial|\psi|^2}{\partial t}\right)\psi = (\nabla-\mathrm{i}\boldsymbol{A})^2\psi+(1-|\psi|^2)\psi, \tag{1}$$

where the parameter $\gamma = 2\tau_E\psi_0/\hbar$ characterizes the chosen material with τ_E being the inelastic collision time and ψ_0 is the value of order parameter at zero temperature and no applied field. This equation should be couple with the equation for the electrostatic potential:

$$\Delta\phi = \mathrm{div}\{\mathrm{Im}[\psi^*(\nabla-\mathrm{i}\boldsymbol{A})\psi]\}, \tag{2}$$

which is the condition for the conservation of the total current in the sample, i.e., $\mathrm{div}\,\boldsymbol{j} = 0$. In Eqs. (1) and (2), all the physical quantities distances are measured in dimensionless units: the coordinates are in units of coherence length $\xi(T)$, time is scaled by Ginzburg–Landau relaxation time t_{GL}=$\pi\hbar/8k_{\mathrm{B}}Tu$, the electrostatic potential ϕ by $\phi_0 = \hbar/2et_{\mathrm{GL}}$, and vector potential $\boldsymbol{A}$ by $H_{c2}\xi$. In these units the magnetic field is scaled by H_{c2}=$\Phi_0/2\pi\xi^2$ (where Φ_0 is the quantum of magnetic flux) and the current density by $j_0 = c\Phi_0/8\pi^2\lambda^2\xi$. Since the width of the considered sample is much smaller than the effective penetration depth we neglected the effect of the current-induced magnetic field and put $\boldsymbol{A} = (-Hy/2, -Hx/2, 0)$. In the present simulations, we take $\xi = 10$ nm and $\lambda = 200$ nm at zero temperature, which are typical values for thin Nb films.[49] In our calculations, the length L and width W of the strip is chosen to be 800 nm and 400 nm, respectively. The grid step is $h_x = h_y = \xi/3$, and the time step is chosen

to be $dt = 0.005t_{GL}$. The slit width S_b is 20 nm. The working temperature T is assumed to be $0.96T_c$. Due to the inhomogeneous distribution of current across the sample, the nature of the PSL solution is strongly dependent on the size of the current lead.[50] We choose the size a of the leads as 100 nm. The distance d_s between the off-centered slit and the centered slit is $L/6$. The external applied current density is $j_e = I/j_0W$. The parameter $u = 5.79$ is in accordance with most low T_c materials[47] and $\gamma = 20$ is assumed for the considered sample. Since we work very close to T_c, heating effects can be neglected in our simulations. Superconductor–vacuum boundary conditions $(\nabla - \mathrm{i}\boldsymbol{A})\psi|_n = 0$, $\nabla\phi|_n = 0$ are taken at boundaries of the sample and normal metal–superconductor boundary conditions $\psi = 0$, $\nabla\phi|_n = -j$ at the current contacts are used in our simulations. We discretized the equations applying finite-difference technique on a uniform 2D Cartesian space grid and use Euler iterative methods to solve the TDGL equation. The equation for the electrostatic potential is solved using the successive over relaxation method. Since the voltage signal in our system is a time-dependent variable, we average the voltage over a time interval to construct the I–V characteristics. The total duration of the simulation depends on the external currents. When no vortices move at the beginning of applied current, the total simulation can be no more than 10^4 time steps. For the slow moving vortices at relatively low currents, the simulation is easy to reach periodical voltage oscillation. In this case, the total duration can be approximately 3×10^4 time steps. While at higher currents, the total duration for the simulation can be up to several millions of time steps due to the multi-harmonic voltage oscillations.

3. Results and discussion

3.1. The effect of slit position on the dynamics of V-Av pair in the absence of magnetic field

Due to the effect of current crowding,[51,52] the transport current flow around the slit will generate positive and negative field in the vicinity of the defect. With increasing current, the positive and negative flux will develop into vortex–antivortex pairs and can be driven off by Lorentz force, which becomes a dynamical system. We demonstrated the dynamics of the V-Av pair depend on the slit position in this part. First of all, we start from the simple dynamical behavior of a current-carrying strip with zero applied field, then the complicated response of the system to transport current and magnetic field will be discussed in next section.

Figure 2 shows the effect of slit location in SC strip on the current-voltage characteristics. The solid line and the dashed line illustrated the current–voltage (I–V) characteristics of the strip contained centered slit and the case of off-centered slit with shifting distance of $d_s = L/6$ from center in SC strip, respectively. For the case with centered slit, the strip keeps superconducting (inset 1) up to the threshold external current density $j_c = 0.24$ (inset 2), at which the SC current density exceeds locally the pair-breaking current j_{GL} and the system turns into a nonequilibrum state.[50] Note that the nonzero slope of the I–V curve is due to the nucleation of the positive and negative flux in the slit and contact resistance from the leads. For the case with off-centered slit, the PSL first appears at the location of the slit as expected (inset 3). The distributions of Cooper-pair density illustrates the distinguishing PSLs for the centered slit and off-centered one. It can be found that the location of the slit have a great impact on the I–V characteristics. The first critical current j_{c1} for the case with off-centered slit is larger than that with centered slit. This is the reason that the order parameter is strongly suppressed in the middle of the strip.[50] However, with further increasing current, the second critical current j_{c2} for the nucleation of new PSL (inset 4) is much smaller for the case with centered slit, since it needs a larger current to reach the condition for the nucleation of next two PSLs.

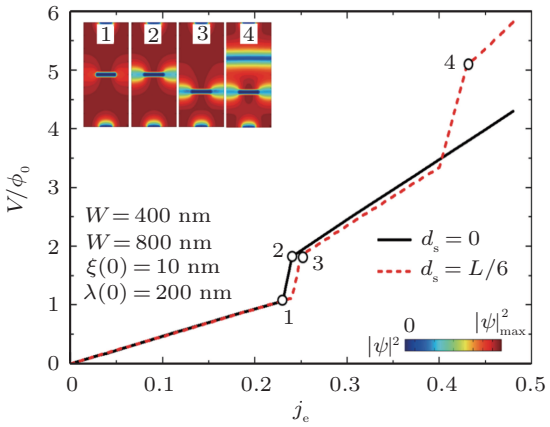


Fig. 2. (color online) Current–voltage characteristics of the sample with the centered-slit (black solid line) and off-centered slit with shift distance $d_s = L/6$ (red dashed line) of slit length $S_a = 2.0$. Panels 1–4 show the Cooper-pair density for current values indicated in the I–V curves.

Figure 3(a) shows the time evolution of output voltage in the sample contained centered (solid line) and off-centered slit (dashed line) at $j_e = 0.4$ and $H = 0$. In order to observe the creation, motion, and disappearance of V-Av pair generated around the slit, we presented the snapshots of magnetic field profile for the two cases at times indicated in the V–t curves. Figure 3(b) shows the development of magnetic field B_z along the line of their motion ($y = L/2$) at different time intervals for the case with centered slit. The average value of the output voltage for the centered slit is larger than the one for the off-centered case. The nucleation of V-Av pairs depends on the slit location. Thus the narrow slit is also an effective phase-slip pinning center, which is like the case of a superconducting stripe with magnetic dots on top.[25] From the periodic oscillations of the voltage, the V-Av pairs are depinned at the minimum of the measured voltage (points 1 and a). With time, the V-Av pairs are separated in opposite directions and travel

towards the lateral edges (insets 2 and b), which leads to the increase of voltage. Then they disappear at the lateral edges of the sample (insets 3 and c). This corresponds to the maximal measured voltage. After the expulsion the SC current is recovered, which results in the decrease of voltage signal. Meanwhile, a new pair of positive and negative flux nucleates again around the slit, and the system relaxes to its initial state (insets 4 and d). Note that we observed only one scenario of dynamical process for different slit lengths in the absence of magnetic field, i.e., the V-Av pair in the slit are both depinned and expelled laterally simultaneously. Nevertheless, in the presence of a weak magnetic field there exists more fascinating phenomena, which will be described in the following section.

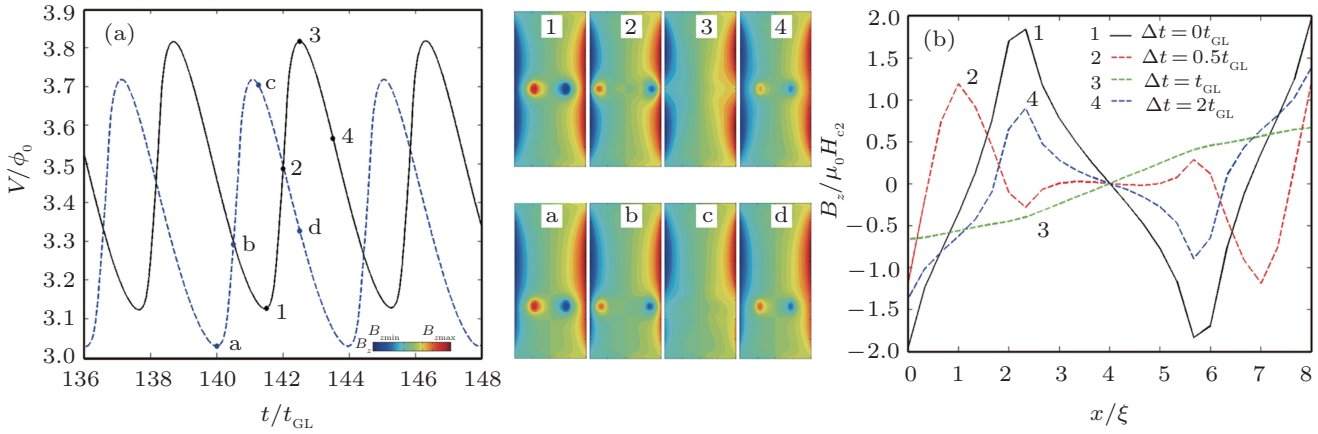


Fig. 3. (color online) (a) Equilibrated voltage vs time responses of the sample contained centered slit (solid line) and off-centered one (dashed line) for $j_e = 0.4$ and $H = 0$. Panels 1–4 [(a)–(d)] show the snapshots of magnetic field profile at times in V-Av pair dynamical process for the centered (off-centered) case. (b) Cross sections of magnetic field profile at $y = L/2$ for the centered case at time intervals indicated in the V–t curves.

3.2. The effect of slit length on the vortex dynamics in the presence of magnetic field

As mentioned above, the dynamics of V-Av not only depends on the slit location in SC strip and mechanical strain, but also depends on the applied magnetic field. The presence of magnetic field break the symmetrical movement of V-Av pairs. Moreover, the lateral vortex will also take part in the dynamical system. For the SC strip containing narrow slit with transport current and applied field will posses complex and fascinating vortex dynamics. In this section, we focus on the response of our system with different slit lengths to increasing applied current for a constant applied magnetic field. The simulations are done within a weak magnetic-field regime so that no Abrikosov vortices enter the sample in the absence of applied current.

The I–V characteristics for two kinds of slit length are shown in Fig. 4(a). The inset snapshots of the Cooper-pair density are illustrated for case of the slit length $S_a = 2.0$. At applied current density $j_e \geq 0.145$, the kinematic vortex (inset 2) is observed on right-hand side and left-hand side by turns till the $j_e \leq 0.186$. When single-side kinematic vortex line appear in the sample, there is no change of slope in the I–V curve. This feature is induced by the low-frequency voltage oscillation (see also Fig. 5(a)), which is similar with our recent work.[44] It should be mentioned that the appearance of kinematic vortex line can lead to a jump of I–V curve in an SC square loop,[37] which is quite different from our results. With further increasing current, phase-slip lines can be observed both on right and left sides of the slit simultaneously. The system is switched into a higher resistive state at the second critical current $j_{c2} = 0.187$, which leads to an abrupt jump and change of the slope of I–V curve. For the case of slit with smaller length, such single-side kinematic vortex lines can be also observed when the applied current density is restricted in the range of $0.23 \leq j_e \leq 0.245$, while the vortex dynamics of V-Av pairs can be distinctly different from the case of longer slit length, which will be explained in the following part in detail. As the current is increased up to $j_{c3} = 0.45$, two new PSLs nucleate at each side of the centered slit (inset 4). This provides for a large jump in the I–V curve. As expected, the critical current j_{c3} for the longer slit length is much smaller.

Figure 4(b) shows the time evolution of output voltage at $j_e = 0.45$, $H = 0.1$. From the periodic multiharmonic voltage oscillation, the two PSLs firstly nucleate at top and bottom side of the centered slit (inset 1). As time goes on, they can be attracted to the two tips of the slit (insets 2) and merge with each other, forming a circular (inset 3) till the superconductivity of region around the slit is utterly suppressed (inset 4). This stage of high voltage can be decreased to the low stage when there are only two PSL at the right and left of the slit (insets 5 and 6). With time, two more vortices nucleate at the top and the bottom side of the centered slit (inset 7), which finally form kinematic PSLs (inset 8). The system relaxes back its initial state to continue the ever dynamical process.

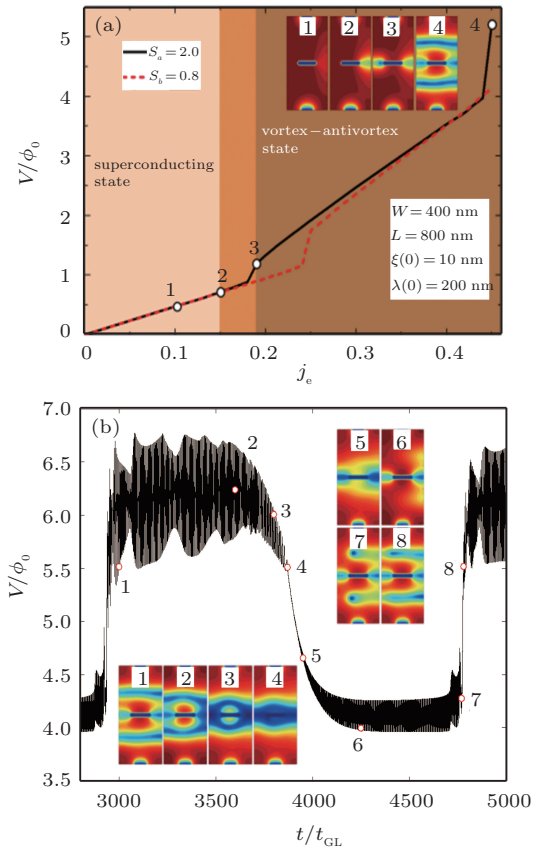


Fig. 4. (color online) (a) Current–voltage characteristics of the sample contained a narrow slit with length $S_a = 2.0$ (black solid line) and with smaller length $S_a = 0.8$ (dashed line) in the current increasing regime for $H = 0.1$. Panels 1–4 shows the inset snapshots of Cooper-pair density indicated in the I–V curve. (b) Equilibrated voltage vs time responses of the sample with centered slit of length $S_a = 2.0$ at $j_e = 0.45$, $H = 0.1$. The insets show the distributions of PSLs at times indicated in the V–t curve.

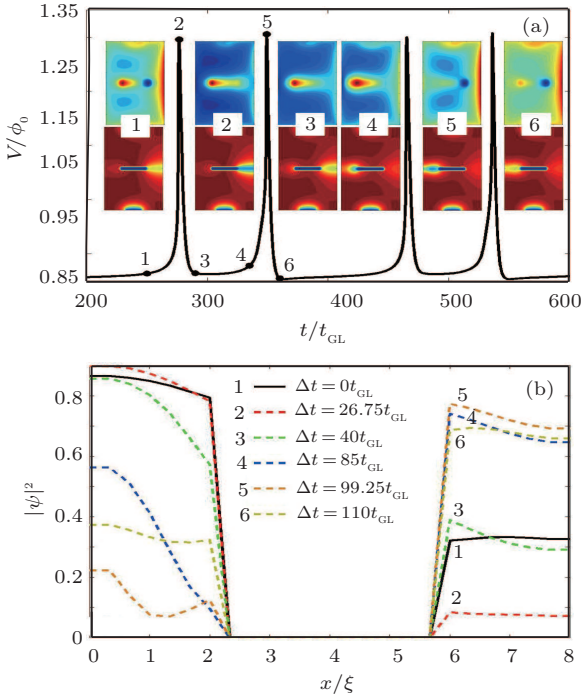


Fig. 5. (color online) (a) Calculated voltage versus time characteristics of the sample for slit length $S_a = 2.0$ at $j_e = 0.18$ and $H = 0.1$. Panels 1–6 show the snapshots of kinematic vortex line at single side by turns. (b) Cross sections of the Cooper-pair density at $y = L/2$ at times indicated in the V–t curve.

Figure 5(a) shows the periodical oscillations of the voltage in the SC strip with slit length $S_a = 2.0$ at $j_e = 0.18$ and $H = 0.1$. To obtain a better insight into the dynamical process of V-Av pair, the snapshots of magnetic field profile and the Cooper-pair density at times indicated in the V–t curve are also plotted. Figure 5(b) illustrates the distribution of the Cooper-pair density along the line of the motion of the V-Av pair. The local flux induced by the current crowding can involve into vortex and antivortex (V-Av). In this case, the slit and the local flux induced by the current crowding promote V-Av generation (vortex-generator), which is similar with the vortices induced by the stray field of the magnetic dots.[30] Since the asymmetric distribution of SC current density around the slit, Lorentz force at right-hand side tip is much stronger, which results in the right-hand side antivortex depined first (inset 1). Then the antivortex travels and disappears at the right lateral edge of the strip (inset 2). This leads to the local maximal voltage. Meanwhile, the right-hand side superconductivity is strongly suppressed so that the right kinematic vortex line appears, while the left of the sample is nearly superconducting (line 2). The remaining vortex in the slit subjected to Lorentz force moves towards the left tip of the slit gradually (inset 3). After the antivortex moving out of the sample, the right-hand side superconductivity is enhanced. At this moment, the left-hand side one starts to be suppressed (line 3). As time goes on, the vortex in the slit comes to the left tip of the slit and the Lorentz force acting on the vortex is larger than the pinning force. In this case, the vortex is depinned and starts to move out from the slit (inset 4). The left-hand side superconductivity of the sample is further suppressed and the right-hand side one is recovered (line 4). Note that the time interval between states 3 and 4 is long enough that the right-hand side superconductivity can be recovered, which implied the frequency of voltage oscillation is quite low. When the vortex travels towards the lateral edge (inset 5) at the global maximal voltage, the left-hand side order parameter is highly suppressed while the right-hand side one recovers back the superconducting state (line 5). After the disappearance of the vortex, a new pair of positive and negative flux was created again (inset 6) at the global minimum of measured voltage. Meanwhile, the suppressed superconductivity at the left-hand side start to enhance gradually (line 6) and it needs time to recover the left-hand side superconductivity (line 1). During this stage, the local flux at the left tip of the slit increases until the right negative flux evolves into moving antivortex for next period. Beyond that the superconductor condensate relaxes toward a new dynamic process. Therefore, such kinematic vortex line appears at single side of the slit by turns periodically.

If the SC strip is under a higher current, the system will exhibit a different dynamic feature from the single-side kinematic vortex state. Figure 6(a) shows the time evolution of

output voltage for the same parameters as in Fig. 5 but at even higher current $j_e = 0.25$. The snapshots of magnetic field profile and Cooper-pair density at times indicated in the V–t curve are also plotted. The dynamical process of such a V-Av pair is described as follows. The antivortex is first depinned (inset 1). Then it travels towards the right lateral edge where it disappears (inset 2). The remaining vortex is depinned under the action of strong Lorenz force (inset 3). After the disappearance of the vortex (inset 4), a new pair of positive and negative flux is created again around the slit (inset 5). Nevertheless, comparing with the case in Fig. 5, the most distinct difference between these two dynamic behaviors is that the time interval between the motion of vortex and antivortex is much smaller than that in Fig. 5, i.e., at the disappearance of the antivortex, immediately the vortex is depinned and travels towards the lateral edge. Due to such small time interval, both the left-hand side and right-hand side order parameter have no enough time to recover its superconducting state. As a consequence, the kinematic vortex lines can be observed both at the right and left sides of the slit simultaneously (see also the snapshots of Cooper-pair density).

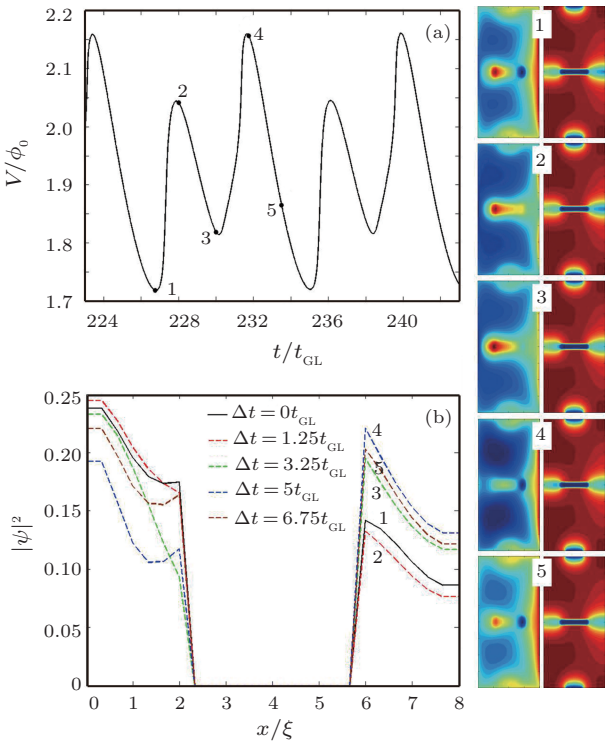


Fig. 6. (color online) Voltage versus time characteristics of the sample for the same parameters as in Fig. 5 but now at the applied current $j_e = 0.25$. Panels 1–5 show the snapshots of phase-slip lines at the double sides of the slit.

The dynamics of V-Av pairs depends not only on the magnitude of applied current, but also on the size of narrow slit. In what follows, we will study the dynamical process of the V-Av pair for two more cases with smaller slit length, which is significantly different from that for longer slit describe above. Figure 7(a) illustrates the voltage vs time characteristics for slit length $S_a = 0.8$ at $j_e = 0.25$ and $H = 0.1$, together with the snapshots of magnetic field profile at times indicated in the V–t curve. In this case, the level of current crowding around the slit is lower than that for the longer one. Therefore, the Lorenz force is not strong enough that the positive and negative flux in the slit is difficult to be depinned. Due to the inhomogeneous distribution of current across the sample, a new vortex also nucleates at the right-hand side lateral edge of the sample under applied drive (inset 1). In view of such conditions, the vortex created at the lateral edge is first depinned and penetrates into the sample (inset 2). Then it travel towards the slit where it is trapped (inset 3) at the local maximum voltage. With time, the vortex in the slit is depinned under the action of large Lorenz force (inset 4) at the local minimal voltage. Then the vortex travels to the lateral edge where it disappears at the maximal voltage (inset 5). Thereafter, a new pair of positive and negative flux nucleate around the slit and the vortex nucleates at the lateral edge (inset 6). In such a dynamical process, it seems that the slit acts as a place for the vortex created at the lateral edge to brake and relax.

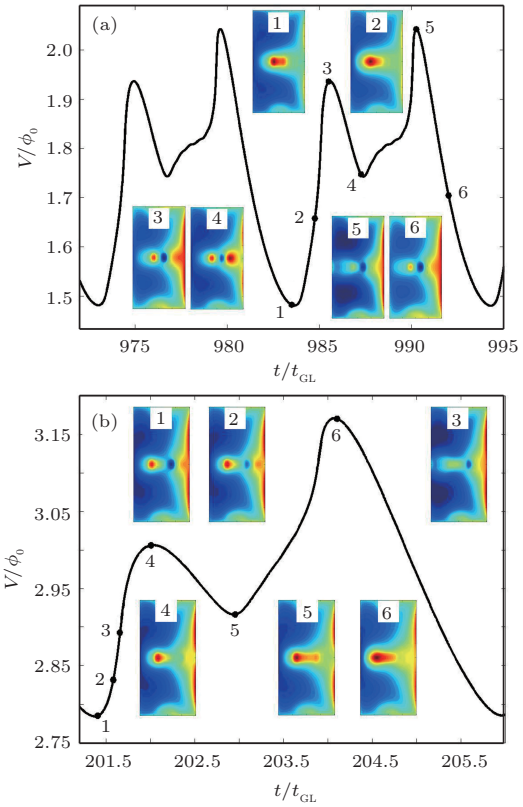


Fig. 7. (color online) (a) Voltage versus time characteristics of the sample for small slit with length $S_a = 0.8$ at $j_e = 0.25$ and $H = 0.1$. Panels 1–6 show the snapshots of dynamics process of lateral vortex. (b) Voltage versus time characteristics for slit with length $S_a = 1.4$ at $j_e = 0.35$ and $H = 0.1$. Snapshots present the dynamics process of V-Av pair and lateral vortex.

In view of this, we conclude that there exists a competition of prior movement between the lateral vortex and V-Av pair in the slit, which gives rise to different dynamical processes. According to the above analysis, we find that the V-Av pair in longer slit takes part in the dynamical process, while

for shorter slit the lateral vortex plays the key role in dynamics system.

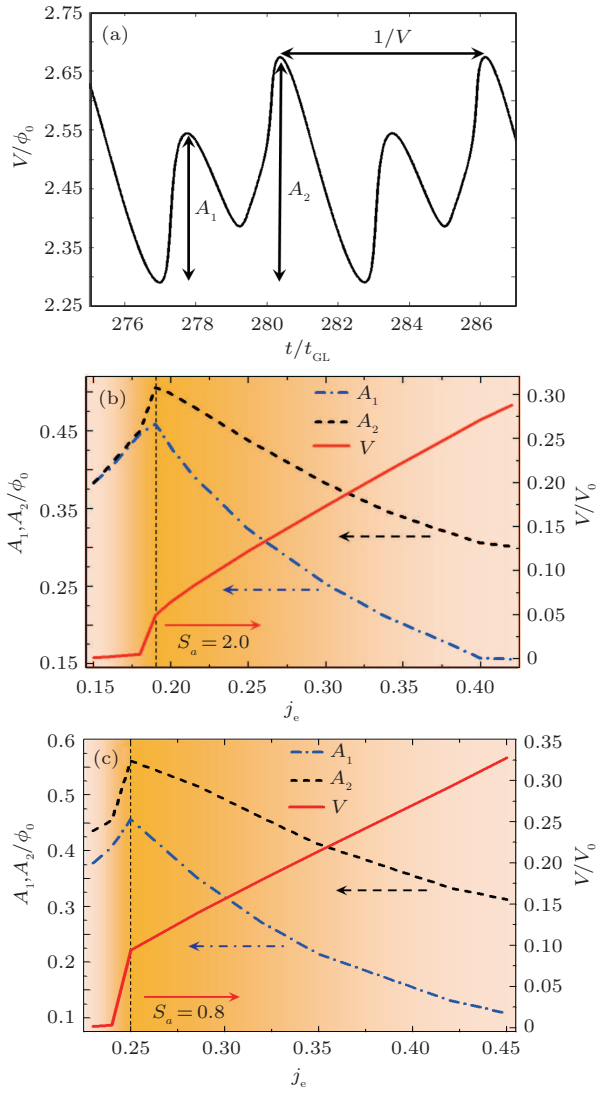


Fig. 8. (color online) (a) Time evolution of voltage of the sample for long slit length $S_a = 2.0$ at $j_e = 3.0$ and $H = 0.1$. (b) Dependencies of the amplitudes A_1 (blue dashed–dotted line, left axis), A_2 (black dashed line, left axis) and frequency (red solid line, left axis) on the applied current density j_e for the slit with length $S_a = 2.0$ at $H = 0.1$. (c) The same parameters as panel (b) but for the slit with length $S_a = 0.8$. The vertical dashed lines are plotted for indicating the transition point.

As a consequence, we can image that there should be a scenario both the V-Av pair in the slit and lateral vortex take part in the dynamical process simultaneously by changing the slit length. Figure 7(b) shows such a dynamical process at $j_e = 0.35$ and $H = 0.1$ for slit length $S_a = 1.4$. We found that the antivortex and lateral vortex are depinned and move towards each other (inset 2). Then they come across and annihilate in the half way between slit and right lateral edge (inset 3). Afterwards, the remaining vortex in the slit will be driven off from the slit (inset 5) and disappears at the left edge of the sample (inset 6). In this sense, the dynamics of V-Av pairs can be tuned by the slit length.

Shown in Fig. 8(a) is the V–t curve for the slit length $S_a = 2.0$ at $j_e = 0.3$ and $H = 0.1$. It can be found that there exists two amplitudes: the smaller one A_1 and the larger one A_2. In order to demonstrate the difference between the quasi-static phase-slip and kinematic phase-slip state, we present the variations of the amplitudes (left axis) and the frequency of voltage oscillation (right axis) as a function of transport current for $H = 0.1$ in Figs. 8(b) ($S_a = 2.0$) and 8(c) ($S_a = 0.8$). The most interesting observation is that the dependencies of the amplitudes on applied currents are not monotonic: they first increase then decrease with the increasing current. The transition current density jet is 0.187 for slit length $S_a = 2.0$, and $j_{et} = 0.246$ for slit length $S_a = 0.8$, which exactly corresponds to the transition point of vortex dynamics from the quasi-static state to kinematic state. Furthermore, from the dependence of frequency on j_e, the frequency is abruptly raised up at the transition point from quasi-static state to kinematic state, which corresponds to the evident jump and change of the slope in the I–V curve. The high frequency oscillation indicated the fast moving vortices at the kinematic phase-slip state. This may give an insight into the distinct difference between these two states.

4. Conclusion

To conclude, using the phenomenological time-dependent Ginzburg–Landau formalism we analyzed the dynamical properties of the vortex–antivortex pair in a current-carrying superconductor film with a narrow slit. We found the slit is an effective phase-slip pinning center and the location of phase slippage in the sample can be predetermined by the location of the slit. When the superconducting strip is under a weak magnetic field, it is surprisingly found that kinematic vortex line appears at the right side or the left side of the slit by turns periodically. This single-side kinematic vortex line attributes to the low-frequency voltage oscillation in the range of low applied currents and weak magnetic field. At higher currents, the phase-slip lines can be observed both at the two sides of the slit due to the fast moving vortex–antivortex pairs. Further increasing applied current, the slit can attract the phase-slip lines and lead to the coalescence of the phase-slip lines during a complicated multiharmonic voltage oscillation. Furthermore, due to the competition between the lateral vortex and the vortex–antivortex pair in the slit, we observed three distinctly different dynamical scenarios of vortex–antivortex depending on slit length. We conjecture that there would exist more dynamical process by adjusting the slit position and external conditions (i.e., applied current and magnetic field). Finally, we analyzed the dependencies of amplitudes and frequency of the voltage oscillations on applied currents for a constant magnetic field. The amplitudes first increase then decrease with increasing applied currents, and the transition point happened to be that from single-side kinematic vortex state to kinematic

vortex–antivortex state. These results may provide explanation for kinematic vortex–antivortex phenomenon and current-voltage characteristics in the sample with artificial defects.

References

[1] Veldhorst M, Molenaar C G, Wang X L, Hilgenkamp H and Brinkman A 2012 *Appl. Phys. Lett.* **100** 072602

[2] Moshchalkov V V, Gielen L, Strunk C, Jonckheere R, Qiu X, van Haesendonck C and Bruynseraede Y 1995 *Nature* **373** 319

[3] Geim A K, Dubonos S V, Lok J G S, Henini M and Maan J C 1998 *Nature* **396** 144

[4] Geim A K, Dubonos S V, Grigorieva I V, Novoselov K S, Peeters F M and Schweigert V A 2000 *Nature* **407** 55

[5] Babic D, Bentner J, Surgers C and Strunk C 2004 *Phys. Rev. B* **69** 092510

[6] Tian M, Wang J, Kurtz J S, Liu Y, Chan M H W, Mayer T S and Mallouk T E 2005 *Phys. Rev. B* **71** 104521

[7] Samoilov A V, Konczykowski M, Yeh N C, Berry S and Tsuei C C 1995 *Phys. Rev. Lett.* **75** 4118

[8] Doettinger S G, Huebener R P, Gerdemann R, Kuhle A, Anders S, Trauble T G and Villegier J C 1994 *Phys. Rev. Lett.* **73** 1691

[9] Xiao Z L, Voss-de Haan P, Jakob G, Kluge T, Haibach P, Adrian H and Andrei E Y 1999 *Phys. Rev. B* **59** 1481

[10] Ivlev B I and Kopnin N B 1984 *Sov. Phys. Usp.* **27** 206

[11] Dmitrenko I M 1996 *J. Low Temp. Phys.* **22** 648

[12] Andronov A, Gordion I, Kurin V, Nefedov I and Shereshevsky I 1993 *Physica C* **213** 193

[13] Sivakov A G, Glukhov A M, Omelyanchouk A N, Koval Y, Müller P and Ustinov A V 2003 *Phys. Rev. Lett.* **91** 267001

[14] Tinkham M 1979 *J. Low Temp. Phys.* **35** 147

[15] Vodolazov D Y and Peeters F M 2007 *Phys. Rev. B* **76** 014521

[16] Chibotaru L F, Ceulemans A, Bruyndoncx V and Moshchalkov V V 2000 *Nature* **408** 833

[17] Misko V R, Fomin V M, Devereese J T and Moshchalkov V V 2003 *Phys. Rev. Lett.* **90** 147003

[18] Geurts R, Milošević M V and Peeters F M 2006 *Phys. Rev. Lett.* **97** 137002

[19] Geurts R, Milošević M V and Peeters F M 2007 *Phys. Rev. B* **75** 184511

[20] Geurts R, Milošević M V and Peeters F M 2009 *Phys. Rev. B* **79** 174508

[21] Carballeira C, Moshchalkov V V, Chibotaru L F and Ceulemans A 2005 *Phys. Rev. Lett.* **95** 237003

[22] Milošević M V, Berdiyorov G R and Peeters F M 2005 *Phys. Rev. Lett.* **95** 147004

[23] Milošević M V and Peeters F M 2004 *Phys. Rev. Lett.* **93** 267006

[24] Milošević M V and Peeters F M 2005 *Phys. Rev. Lett.* **94** 227001

[25] Milošević M V and Peeters F M 2006 *Physica C* **437–438** 208

[26] Milošević M V, Gillijns W, Silhanek A V, Libál A, Peeters F M and Moshchalkov V V 2010 *Appl. Phys. Lett.* **96** 032503

[27] Berdiyorov G R, Milošević M V and Peeters F M 2009 *Phys. Rev. B* **80** 214509

[28] Kapra A V, Misko V R, Vodolazov D Y and Peeters F M 2011 *Supercond. Sci. Technol.* **24** 024014

[29] Gladilin V N, Tempere J, Devreese J T, Gillijns W and Moshchalkov V V 2009 *Phys. Rev. B* **80** 054503

[30] Lange M, J Van Bael Margriet, Bruynseraede Yvan and Moshchalkov V V 2003 *Phys. Rev. Lett.* **90** 197006

[31] Milošević M V and Peeters F M 2005 *Europhys. Lett.* **70** 670

[32] Gillijns W, Milošević M V, Silhanek A V, Moshchalkov V V and Peeters F M 2007 *Phys. Rev. B* **76** 184516

[33] Silhanek A V, Gillijns W, Milošević M V, Volodin A, Moshchalkov V V and Peeters F M 2007 *Phys. Rev. B* **76** 100502

[34] Silhanek A V, Gladilin V N, Van de V J, Raes B, Ataklti G W, Gillijns W, Tempere J, Devreese J T and Moshchalkov V V 2011 *Supercond. Sci. Technol.* **24** 024007

[35] Lange M, Van B M J, Silhanek A V and Moshchalkov V V 2005 *Phys. Rev. B* **72** 052507

[36] Lisboa Filho P N, de Souza Silva C C and Cabral L R E 2009 *Phys. Rev. B* **80** 012506

[37] Berdiyorov G R, Milošević M V and Peeters F M 2010 *Physica C* **470** 946

[38] Zha G, Peeters F M and Zhou S 2014 *Europhys. Lett.* **108** 57001

[39] Berdiyorov G R, Milošević M V, Covaci L and Peeters F M 2011 *Phys. Rev. Lett.* **107** 177008

[40] Jelić Ž L, Milošević M V, Van de V J and Silhanek A V 2015 *Sci. Rep.* **5** 14604

[41] Jelić Ž L, Milošević M V and Silhanek A V 2016 *Sci. Rep.* **6** 35687

[42] Carapella G, Sabatina P, Barone C, Pagano S and Gombos M 2016 *Sci. Rep.* **6** 35694

[43] Carapella G, Pagano S and Gombos M 2017 *Supercond. Sci. Technol.* **30** 025018

[44] He A, Xue C, Yong H and Zhou Y 2016 *Supercond. Sci. Technol.* **29** 065014

[45] Silhanek A V, Milošević M V, Kramer R B G, Berdiyorov G R, Van de V J, Luccas R F, Puig T, Peeters F M and Moshchalkov V V 2010 *Phys. Rev. Lett.* **104** 017001

[46] Adami O-A, Jelić Ž L, Xue C, Abdel-Hafiez M, Hackens B, Moshchalkov V V, Milošević M V, Van de V J and Silhanek A V 2015 *Phys. Rev. B* **92** 134506

[47] Kramer L and Watts-Tobin R J 1978 *Phys. Rev. Lett.* **40** 1041

[48] Watts-Tobin R J, Krähenbühl Y and Kramer L 1981 *J. Low Temp. Phys.* **42** 459

[49] Gubin A I, Ilin K S, Vitusevich S A, Siegel M and Klein N 2005 *Phys. Rev. B* **72** 064503

[50] Berdiyorov G R, Milošević M V and Peeters F M 2009 *Phys. Rev. B* **79** 184506

[51] Berdiyorov G R, Milošević M V and Peeters F M 2012 *Appl. Phys. Lett.* **100** 262603

[52] Adami O A, Cerbru D, Cabosart D, Motta M, Cuppens J, Ortiz W A, Moshchalkov V V, Hackens B, Delamare R, Van de Vondel J and Silhanek A V 2013 *Appl. Phys. Lett.* **102** 052603